

Fragmentation in the eikonal picture

R. Blankenbecler*

Stanford Linear Accelerator Center, Stanford, California 94305

J. R. Fulco† and R. L. Sugar†

Department of Physics, University of California, Santa Barbara, California 93106

(Received 30 July 1973)

The eikonal approach to the scattering and production of high-energy particles is reviewed and extended. Several models for the high-energy behavior of the eikonal phase are discussed. We show how to introduce effects associated with the fragmentation of the incident particles into the eikonal framework, and indicate how these effects can influence the energy dependence of cross sections. The contributions of the triple-Regge region of phase space to the amplitude are examined. The importance of absorptive effects is clearly shown by demonstrating that the sign of the term linear in the triple-Pomeron coupling is negative in the total cross section.

I. INTRODUCTION

The eikonal approach to scattering at short wavelengths has been very useful in a wide variety of applications ranging from classical wave propagation to ultrahigh-energy physics. The purpose of this paper is to give a brief review of the physical insight that has been gained concerning strong-interaction processes at high energies and to underline the theoretical questions that remain.

One of the main virtues of the eikonal method is that the geometrical constraints of unitarity are automatically enforced on the elastic scattering amplitude. In fact it has been possible to construct eikonal models for which the scattering operator satisfies full multiparticle unitarity in the direct channel.¹⁻⁵ The approach is general enough to allow one to study a variety of production mechanisms.

In the relativistic domain the eikonal approximation has been studied most thoroughly for elastic scattering at high energies and small momentum transfers. The two incident particles are pictured as propagating through the interaction region in a straight line without making appreciable fractional changes in their energies or longitudinal momenta. It has been possible to show that this picture is correct for certain classes of Feynman diagrams. The case in which the incident particles interact via the exchange of elementary particles [see Fig. 1(a)] has been extensively studied.⁶⁻⁹ This simplest of all exchange models can even be extended to large momentum transfers.^{9,10} Tiktopoulos and Treiman¹¹ have shown that while an eikonal-like formula does result when vector mesons are exchanged, this is not the case in the exchange of scalar mesons. In the latter case the large mo-

menta of the incident particles can be transferred to the exchanged quanta in violation of the eikonal picture. This does not happen for vector exchange to leading order in s .

The much more complicated problem involving the exchange of noninteracting towers in quantum electrodynamics (QED) has been studied by Cheng and Wu.¹² This work led to their well-known model of high-energy scattering.¹³ The related problem of the exchange of noninteracting ladders in ϕ^3 theory [see Fig. 1(b)] has also been studied extensively.^{14,15} This work allows one to correctly treat the Mandelstam cuts which arise when multiple exchanged ladders are intertwined along the projectile and target lines. For the exchange of one or two ϕ^3 ladders, the leading asymptotic behavior of the Feynman graphs does come when the large momenta follow the eikonal paths. However, for the exchange of three or more ladders, the leading asymptotic behavior again comes from short-circuit paths.¹⁵

The exchange of interacting ladders and of nonplanar checkerboard graphs [see Fig. 1(c)] has also been studied.^{3,4,16} These calculations indicate that interactions among the exchanged ladders or towers can be important. In general the forces between N -exchanged bosons do not saturate, and the binding increases faster than N . The consequences of this will be discussed in Sec. II.

The simple eikonal picture in which the two incident particles retain their identity throughout the scattering process is made plausible by the leading-particle effect, but it is obviously highly oversimplified. Recently Skard and Fulco¹⁷ have extended the eikonal model to include effects associated with the fragmentation of the incident particles. Their work demonstrates a very interesting

new physical point—namely, that the presence of fragmentation channels in black-disk scattering can make the disk overblack and thereby induce transparency in the system. This unexpected effect will be discussed in Sec. III, within a general framework. When the eikonal phase is dominated by Regge-pole exchange, fragmentation effects play a crucial role in determining the triple-Regge contribution to cross sections. This subject is also briefly discussed in Sec. III.

II. ABSORPTION—NO FRAGMENTATION OR DIFFRACTION

The conventional eikonal form for the invariant elastic scattering amplitude M is

$$M(s, t) = 4\pi i s \int_0^\infty b db J_0(b\sqrt{-t})(1 - e^{i\chi(b, s)}), \quad (1)$$

where the complex phase $\chi(b, s)$ is the sum over all connected graphs involving the exchange of an arbitrary number of mesons as shown in Fig. 2.¹⁸ By connected graphs we mean that the circles in Fig. 2 represent connected t -channel scattering amplitudes. Disconnected graphs arise from the expansion of the exponential. It is probably best to regard Eq. (1) as a simple ansatz which automatically takes into account the constraints of unitarity. This equation can be “derived” from Feynman graphs of the type shown in Fig. 2 (see Ref. 18), provided one considers only the contributions in which the incident particles retain their large mo-

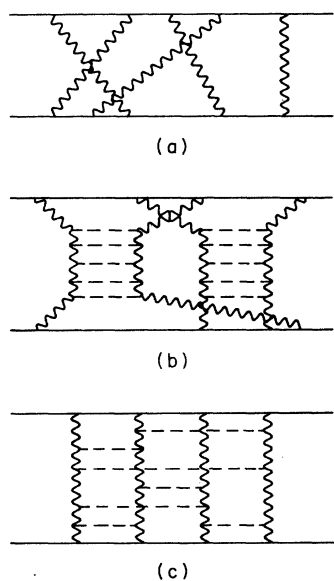


FIG. 1. (a) Typical elementary particle exchange graph in the eikonal approximation. (b) Sample non-interacting ladder graph. (c) Nonplanar checkerboard graph.

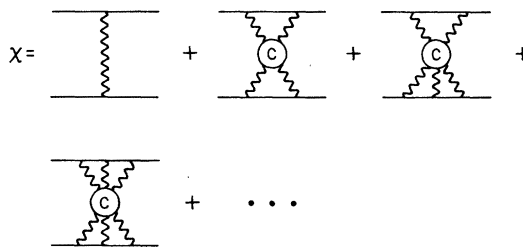


FIG. 2. Connected exchanges which contribute to eikonal phase.

menta throughout the scattering process.¹⁹ However, as was pointed out in the Introduction, these contributions do not always give the leading asymptotic behavior of the individual Feynman graphs.

In general the circles in Fig. 2 can correspond to $n \rightarrow m$ meson scattering amplitudes; however, in all of the work that we are aware of only diagonal ($n \rightarrow n$) contributions to χ have been taken into account. While it should be possible to discuss the eigenchannels in the t channel, we shall limit ourselves to diagonal terms only. It is then convenient to write

$$i\chi(b, s) = \sum_{n=1}^{\infty} i^n d_n(b, s) s^{[n(\alpha-1) + a(n)]} e^{-n\mu b}. \quad (2)$$

Here n is the number of mesons being exchanged, μ is their mass, and α is their spin. We have explicitly displayed the factor of $e^{-n\mu b}$ since for n -meson exchange the nearest t -channel singularity is at $t = (n\mu)^2$.²⁰ As a result, we expect $d_n(b, s)$ to go to a constant for large b and fixed s . We also expect that for large s , $a(n)$ can be chosen so that $d_n(b, s)$ varies with s , at most, like a power of $\ln s$. This is the case for the diagrams considered in Refs. 12–16.

Cheng and Wu have suggested that for large values of b , terms in Eq. (2), which correspond to the exchange of three or more mesons, can be neglected because of their more rapid fall off. Let us therefore start by considering the first two terms in Eq. (2). In general d_1 is real, $\text{Re} d_2 > 0$, and $a(2) > 0$. As a result, for large values of s and b the ladder or tower graphs dominate the single particle exchange terms for vector exchange. They also dominate for scalar exchange provided $a(2) > 1$. If one retains only the contributions to χ arising from the tower graphs, then for vector exchange $e^{i\chi(b, s)}$ goes to zero at large s for $b \leq [a(2)/2\mu] \ln s \equiv R_0 \ln s$ and goes to 1 for $b > R_0 \ln s$. In the present normalization the total and elastic cross sections at high energies are given by

$$\sigma_T = 4\pi \int_0^\infty b db \text{Re}(1 - e^{i\chi(b, s)}) \quad (3)$$

and

$$\sigma_{el} = 2\pi \int_0^\infty b db |1 - e^{i\chi(b,s)}|^2. \quad (4)$$

So for vector exchange¹³

$$\sigma_T = 2\sigma_{el} \approx 2\pi(R_0 \ln s)^2. \quad (5)$$

A similar result holds for scalar exchange when $a(2) > 2$.¹⁴ The only change is that $R_0 = [a(2) - 2]/2\mu$. Equation (5) of course corresponds to scattering from a black disk of radius $R_0 \ln s$.

Whether the contributions to χ arising from the exchange of three or more mesons can actually be neglected for large b depends upon the behavior of $a(n)$ as a function of n . In the checkerboard graph model [see Fig. 1(c)] $a(n)$ grows like $\frac{1}{2}n(n-1)$,^{3,16} so these terms obviously cannot be neglected. This behavior for $a(n)$ is not hard to understand. The particles represented by dashed lines in Fig. 1(c) give rise to attractive forces among the exchanged mesons. Since the number of "two-body potentials" increases like $\frac{1}{2}n(n-1)$, it is hardly surprising that the binding among the mesons does also. In this case the series for $i\chi$ is marginally convergent. For most values of the input parameters the total and elastic cross sections fall like a power of energy as s goes to infinity.

These checkerboard graph models were simplified versions of multiperipheral-type theories in which the approximations were tailored to be accurate in the multi-Regge region of phase space. The results show that these contributions are then strongly suppressed by a type of self-damping imposed by unitarity. This suppression of large relative energies between secondaries is required by the experimental data.

Models which include many-body forces among the exchanged mesons (see Fig. 3) have also been studied.⁴ The results are qualitatively similar to those obtained in the checkerboard model, except that there is a limited range of input parameters for which the multichain forces saturate, i.e., for which $a(n)$ grows less rapidly than n . In the latter case the multimeson exchange contributed to χ can of course be neglected.

The behavior of $a(n)$ in relativistic field theories remains an open question. Three cases can be

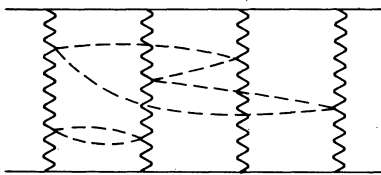


FIG. 3. Many-body forces.

identified:

(1) $a(n)$ grows less rapidly than n . In this case only the one- and two-meson exchange contributions are important at large b . As a result, for vector exchange there is always appreciable scattering out to b of order $R_0 \ln s$, and Eq. (5) holds.

(2) $a(n)$ grows more rapidly than n . Here all terms in the series for χ must be retained and a detailed calculation is necessary to determine the high-energy behavior of the total cross section. This case is further complicated by the fact that couplings between the various meson channels are likely to be important.

(3) $a(n)$ grows like n . In this case the high-energy behavior depends critically on the behavior of the d_n . For example, if $d_n \approx d^n/n!$, then one again obtains black-disk scattering for vector exchange, while if $d_n \approx d^n$ one finds that for vector exchange

$$i\chi(b, s) = ide^{-\mu b}(1 - ids^a e^{-\mu b})^{-1}. \quad (6)$$

Here we have written $a(n) = (n-1)a$, since by definition $a(1) = 0$. The first two terms in the series expansion of Eq. (6) agree with the results of Cheng and Wu, but this form for χ leads to a total cross section which falls like a power of the energy.

The high-energy behavior of $\chi(b, s)$ depends critically on the mechanism for producing particles in the central region. Particle production can be studied in the eikonal framework by treating $\chi(b, s)$ as an operator.¹⁻⁵ In general it is a functional of the creation and annihilation operators of the produced particles. In Refs. 3-5, where the form of $\chi(b, s)$ is taken from the multiperipheral model, $\chi(b, s)$ turns out to be an unbounded operator for most values of the input parameters. It is then hardly surprising that one must take into account all powers of $\chi(b, s)$ when computing the scattering amplitude. However, it is also possible to construct reasonable models for which $\chi(b, s)$ is a bounded operator.^{4,21} In these models it is possible to adjust the input parameters so that the tower-dominance hypothesis holds. It is also possible to arrange for any desired energy dependence for the total cross section.

III. FRAGMENTATION AND DIFFRACTION

Although the simple eikonal picture discussed in Sec. II is quite appealing, it certainly cannot be the whole story. If the incident particles never lost a significant fraction of their momenta, then all of the produced particles would have to be produced in the pionization region. Experimentally, one knows that the incident particles often fragment into two or more secondaries which share the large incident momentum. Such effects are present in some of the Feynman-diagram models we have

mentioned. For example, the diagrams which correspond to the exchange of one or two ϕ^3 ladders only give rise to the simple eikonal picture if one treats the ladders in the leading-log approximation. These diagrams also contain terms in which intermediate particles share the large incident momenta. Such terms, which break the eikonal picture, contribute to nonleading powers of lns. A similar result undoubtedly holds for the exchange of QED towers.

Fragmentation effects can be included in the general eikonal picture provided the invariant mass of the fragments of each particle is small compared to the total center-of-mass energy.^{2,17} It is convenient to divide both the intermediate and final states into two classes: those in which there are no large-rapidity gaps and those in which there is at least one large gap. For simplicity we consider explicitly only those final states in which there is at least one large gap.²² Then the scattering amplitude can be written in matrix form²³

$$M_{kl}(s, t) = 4\pi i s \int_0^\infty b db J_0(b\sqrt{-t})(1 - e^{i\chi(b, s)})_{kl}, \quad (7)$$

where the subscripts label the various states with at least one large-rapidity gap. They consist of the incident state and all states to which it can be diffractively excited. Typical diagrams are shown in Fig. 4. The phase χ , which is represented by a wavy line in Fig. 4, is itself a sum of diagrams in which none of the intermediate states have large rapidity gaps. We assume that these nondiffractive intermediate states produce absorption in all the eigenchannels and therefore write

$$i\chi_{kl}(b, s) = -A_{kl}(b, s), \quad (8)$$

where A is taken to be a positive definite Hermitian matrix which can be diagonalized by the unitary matrix $G(b, s)$:

$$\begin{aligned} [G^{-1}(b, s)A(b, s)G(b, s)]_{kl} &= \Lambda_{kl} \\ &= \delta_{kl} a_k(b, s). \end{aligned} \quad (9)$$

The scattering amplitude is then given by

$$\begin{aligned} M_{jl}(s, t) &= 4\pi i s \int_0^\infty b db J_0(b\sqrt{-t}) \\ &\quad \times \sum_k G_{jk}(b, s)(1 - e^{-a_k(b, s)}) \\ &\quad \times G^{-1}_{kl}(b, s). \end{aligned} \quad (10)$$

One cannot go much further without making specific dynamical assumptions. However, it is amusing to consider specific classes of possible behavior. Suppose that there are N discrete eigenvalues of A which are very large out to be an im-

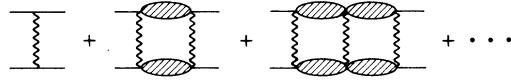


FIG. 4. Typical fragmentation graphs.

perfect parameter of order b_0 (perhaps $b_0 \sim R_0 \ln s$) and that all of the eigenvalues decrease rapidly to zero for $b > b_0$. Then, assuming that $G(b, s)$ is a slowly varying function of b , one sees that

$$\begin{aligned} \sigma_T^j &= \frac{1}{s} \text{Im} M_{jj}(s, 0) \\ &\approx 4\pi \int_0^{b_0} b db \sum_{l=n}^N |G_{jl}(b, s)|^2 \approx 2\pi b_0^2 g_{jj}, \end{aligned} \quad (11)$$

$$\begin{aligned} \sigma_{el}^j &= 2\pi \int_0^\infty b db |(1 - e^{-A})_{jj}|^2 \\ &\approx \pi b_0^2 |g_{jj}|^2, \end{aligned} \quad (12)$$

and

$$\begin{aligned} \sigma^{jk} &= 2\pi \int_0^\infty b db |(1 - e^{-A})_{jk}|^2 \\ &\approx \pi b_0^2 |g_{jk}|^2, \end{aligned} \quad (13)$$

where

$$g_{jk} = \sum_{l=n}^N G_{jl}(b_0, s) G_{kl}^*(b_0, s). \quad (14)$$

Notice that as long as there is more than one diffractive channel the total cross sections do not all have to approach the same limit as they would in the simple black-disk-eikonal models discussed in Sec. II. Furthermore, since $g_{jj} \leq 1$, we see that $\sigma_{el}/\sigma_T \leq \frac{1}{2}$ instead of being exactly $\frac{1}{2}$ as in the simple black-disk models. However, if we define the diffractive cross section by

$$\sigma_{dif}^j = \sigma_{el}^j + \sum_{k \neq j} \sigma^{jk}, \quad (15)$$

then we obtain the important result¹⁷

$$\sigma_{dif}^j = \frac{1}{2} \sigma_T^j. \quad (16)$$

The energy dependence of the various cross sections depends in detail on the behavior of b_0 and the $g_{ij}(s)$.

There are two special cases of interest. First, if all of the eigenvalues of A are large out to $b \approx b_0$, then $g_{jk} = \delta_{jk}$. So, $\sigma_T^j \approx 2\sigma_{el}^j \approx 2\pi b_0^2$ and σ^{jk}/σ_T^j goes to zero at high energies. These are just the results of the one channel model. Going to the opposite extreme consider the case in which only one eigenvalue of A is large out to $b \approx b_0$. This is equivalent to taking A to be separable, so we write

$$A_{kl}(b, s) \equiv G_k(s) a(b, s) G_l(s). \quad (17)$$

This is a crude version of the model discussed in Ref. 17. Writing $\sum_R G_R^2(s) = I(s)$, we see that the scattering amplitude takes the form

$$M_{Rl}(s, t) = 4\pi i s \int_0^\infty b db J_0(b\sqrt{-t}) \frac{G_R(s)G_l(s)}{I(s)} \times (1 - e^{-I(s)a(b,s)}). \quad (18)$$

In general, the functions G_R and $I(s)$ depend on the impact parameter b . On the basis of our previous comments we expect $a(b, s)$ to grow like a power of s for fixed b . $I(s)$ will also increase with s since new diffractive channels are continually being opened, but we would not expect it to grow nearly as rapidly as $a(b, s)$. In that case the value of b_0 is only slightly affected, actually only logarithmically, by the presence of the diffractive channels; however, the factor of $I(s)^{-1}$ under the integral in Eq. (18) means that these channels tend to make the disk more transparent. In the work of Skard and Fulco,¹⁷ fragmentation effects are treated in a manner similar to the diffraction model.²⁴ They find that $I(s)$ grows like $(\ln s)^\eta$, where η is constrained to vary between 0 and 2 by self-consistency requirements. Therefore, in this model the disk is no longer black and the total cross section behaves like $(\ln s)^{2-\eta}$. The value of η depends on the details of the fragmentation mechanism. It can even be a slowly varying function of s .

Finally, let us consider the effects of fragmentation and absorption in a multiperipheral-like model. The simplest diagrams that contribute to the eikonal phase are shown in Fig. 5(a). Cutting these diagrams, one can, of course, divide the intermediate states into those with no large-rapidity gaps and those with one or more such gaps. Examples are shown in Fig. 5(b) and 5(c), respectively. The wavy lines represent ladders whose high-energy behavior is assumed to be dominated by a Regge pole, with intercept close to or equal to 1. For the graphs in Fig. 5(b), these Regge poles give rise to absorptive corrections to the basic multiperipheral production amplitude. Notice that the one-gap contributions are necessarily closely related to the zero-gap ones because the same graphs contribute to both.

The graphs in Fig. 5(b) which have absorptive corrections (wavy lines) interfere destructively with the graph obtained by cutting the simple ladder. The graph in which the Reggeon is attached to the incoming lines and the one in which it is attached to the outgoing lines both contribute to the two-Reggeon cut. Each of these graphs is equal in magnitude but opposite in sign to the AFS graph¹⁵ [the first one in Fig. 5(c)] which has one large-rapidity gap. This is the origin of the well-known result that in the eikonal model the two-Reggeon cut

makes a negative contribution to the total cross section. The same sign reversal holds for the triple-Regge term which also makes a negative contribution to the total cross section. The physical interpretation of the sign reversal is simple and clear. If fragmentation is caused by a predominantly absorptive exchange, such as the Pomeron, its lowest-order contribution to the total cross section is negative, whereas if it is caused by a real exchange, the resulting contribution is positive.²⁵ This is related to the familiar theorem in multichannel potential scattering that a Hermitian transition potential produces attraction below threshold and, to its forgotten corollary, that an anti-Hermitian one leads to repulsion.

The close connection between the Mandelstam cut and the triple-Regge contribution is illustrated in Fig. 6. If no rungs are allowed in the bottom ladder, this diagram is exactly the two-Reggeon cut. In both cases the sign obtained in the eikonal model is in agreement with that obtained in Gribov's Reggeon calculus.²⁶ The existence of certain canceling graphs for the triple-Regge terms has been discussed in perturbation theory

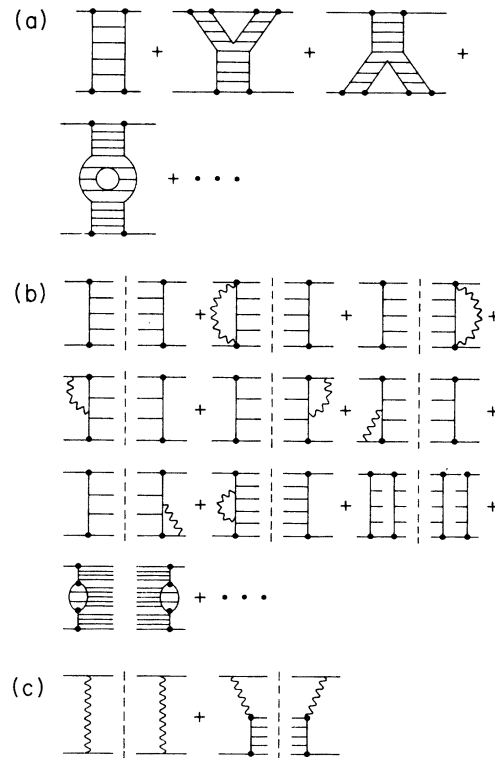


FIG. 5. (a) Interacting ladder-type contributions to the eikonal phase. (b) Lowest-order absorptive corrections to the zero-gap contribution. (c) Lowest-order fragmentation graphs.

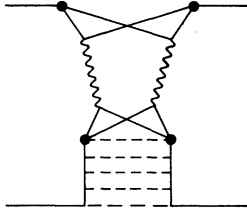


FIG. 6. An illustration showing the close connection between the triple-Regge and the Mandelstam graphs.

in the excellent paper by Halliday and Sachrajda.²⁷

The diffractive production of large-mass fragmentation states has been extensively studied because of their connection to the triple-Pomeron vertex function.^{28,29} One usually assumes that the dominant production mechanism is via the exchange of a simple factorizable Pomeranchuk pole as in the second graph of Fig. 5(c). In the eikonal picture this assumption is highly questionable. If M is the mass of the fragmentation state, then the Pomeranchuk (radius)² of the process is of order $\alpha' \ln(s/M^2)$. Since the region of interest for the decoupling theorems is $M^2 \approx \epsilon s$, where ϵ is fixed, only small values of the impact parameter are important. It is this region of large M^2 in the integration which gives rise to a contribution to the total cross section, which increases with energy. However, it is just for these values of the impact parameter that shadowing and absorption effects should be most important. These absorption interactions all have (ranges)², which can be as large as $\alpha' \ln s$. They will be important and will tend to suppress the contribution of this region of phase space.³⁰ In fact, we have seen that some of the simple diagrams of Fig. 5(b) actually reverse its sign. When higher-order terms in the eikonal expansion are retained, the total cross section does not become negative but falls as a function of s . Whether additional absorption effects such as those depicted in Fig. 7 actually eliminate the inconsistency of a nonvanishing triple-Pomeranchuk coupling is not clear. However, it certainly seems important to take the effects of unitarity into account, particularly at the small impact parameters that are important in the large-mass triple-Regge region.

A preliminary calculation of the single diffractive excitation (or Y graph) has been performed. Be-

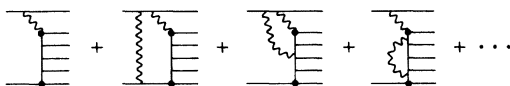


FIG. 7. Absorptive corrections to the fragmentation graphs.

cause of the shadowing effect, the net first-order contribution of the triple-Pomeron vertex to the total cross section is negative. However, the contribution to the inclusive cross section is in complete agreement with that obtained in the Mueller approach.²⁹ The result is that $I(b, s)a(b, s)$ [refer to Eq. (18)] grows like $\ln \ln s$ for $b^2/\ln s$ fixed and this produces a total cross section which falls as $(\ln \ln s)^{-1}$. If the triple Pomeron decouples, then the total cross section approaches a constant. In either case, however, the result is consistent. Higher-order diffractive contributions will change this result and the rate of fall of the total cross section, but it certainly demonstrates that it is important to treat the effects of shadowing and absorption in the triple-Regge region.

IV. CONCLUSION

The eikonal approach to high-energy scattering and particle production has many attractive features; in particular the constraints of s -channel unitarity are built in from the start. Furthermore, one ordinarily obtains a simple physical picture in the impact parameter representation, no matter how complicated the l -plane structure of the scattering amplitude is. The approach is general enough to incorporate any energy dependence of the total cross section (consistent with the Froissart bound) and to allow one to study a variety of production mechanisms. The generality of the approach is also a disadvantage since all of the specific predictions are quite model-dependent and can be changed by altering the form of the eikonal phase. A second drawback is that the constraints of t -channel unitarity are not automatically incorporated, and in general it appears to be difficult to include them.

Although a great deal of work has gone into this subject, a large number of open questions remain. Probably the most important is the behavior of the eikonal phase $\chi(b, s)$ for large values of b and s . If the tower-dominance assumption of Cheng and Wu

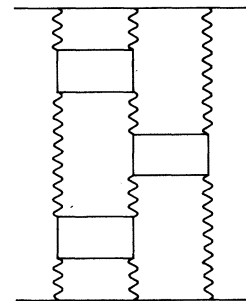


FIG. 8. Three-photon tower graph.

is correct, then in quantum electrodynamics $\chi(b, s)$ is large out to impact parameters of order lns. A similar result would hold if the asymptotic behavior of $\chi(b, s)$ were dominated by a Regge pole with intercept greater than one. Calculations of the checkerboard graphs cast doubt on the tower-dominance hypothesis; however, these calculations have not been done in the framework of QED. It would be particularly interesting to know the asymptotic behavior of the QED graphs corresponding to the exchange of three interacting photons. An example of such graphs is shown in Fig. 8. If the checkerboard graph calculations are an accurate guide then these graphs should give a contribution to $\chi(b, s)$, which is important out to larger impact parameters than the tower-graph contribution.

We have seen in Sec. III that once fragmentation effects are taken into account, the eikonal phase $\chi(b, s)$ is in general an operator. In this case the energy dependence of the total cross section depends crucially on the details of the fragmentation mechanism. For example, the fact that some of the eigenvalues of $\chi(b, s)$ are large out to an impact parameter of order lns does not necessarily mean that the Froissart bound is saturated. The diffrac-

tive channels tend to make the disk transparent and therefore decrease the size of the total cross section, which could then have any asymptotic behavior consistent with s -channel unitarity.

The effect of absorption on the triple-Regge region of phase space was shown to be physically necessary and mathematically important. The usual derivation of the decoupling theorems is particularly sensitive to these effects. Both the sign and magnitude of the terms linear in the triple-Pomeron coupling constant can be strongly modified. The sign-reversal phenomenon was shown to be closely related to the same effect occurring in the AFS-Mandelstam discussion of the two-Pomeron cut. In fact, the triple-Regge region and the two-Pomeron cut were shown to arise from the same type of diagrams and one is the limit of the other.

In summary, we have seen that the eikonal approach offers many advantages in that it builds in the constraints of unitarity and affords a simple picture of scattering and production processes in impact-parameter space. However, as in all relativistic theories, high-order effects are important, especially at high energies, and the expected asymptotic behavior in the energy is not yet known rigorously for any realistic model.

*Work supported by the U. S. Atomic Energy Commission.

†Work supported by the National Science Foundation.

¹G. Calucci, R. Jengo, and C. Rebbi, *Nuovo Cimento* **4A**, 330 (1971); **6A**, 601 (1971).

²R. Aviv, R. Blankenbecler, and R. Sugar, *Phys. Rev. D* **5**, 3252 (1972).

³S. Auerbach, R. Aviv, R. Blankenbecler, and R. Sugar, *Phys. Rev. Lett.* **29**, 522 (1972); *Phys. Rev. D* **6**, 2216 (1972).

⁴R. Sugar, *Phys. Rev. D* **8**, 1134 (1973).

⁵S. Auerbach, U. C. Berkeley report (unpublished).

⁶S.-J. Chang and S. Ma, *Phys. Rev. Lett.* **22**, 1334 (1969); *Phys. Rev.* **188**, 2385 (1969).

⁷H. Cheng and T. T. Wu, *Phys. Rev.* **186**, 1611 (1969).

⁸H. D. I. Abarbanel and C. I. Itzykson, *Phys. Rev. Lett.* **23**, 53 (1969).

⁹M. Lévy and J. Sucher, *Phys. Rev.* **186**, 1656 (1969).

¹⁰R. Blankenbecler and R. Sugar, *Phys. Rev. D* **2**, 3024 (1970).

¹¹G. Tiktopoulos and S. B. Treiman, *Phys. Rev. D* **3**, 1037 (1971).

¹²H. Cheng and T. T. Wu, *Phys. Rev. D* **1**, 2775 (1970).

¹³H. Cheng and T. T. Wu, *Phys. Rev. Lett.* **24**, 1456 (1970).

¹⁴S.-J. Chang and T.-M. Yan, *Phys. Rev. Lett.* **25**, 1586 (1970); *Phys. Rev. D* **4**, 537 (1971).

¹⁵B. Hasslacher *et al.*, *Phys. Rev. Lett.* **25**, 1591 (1970); G. M. Cicuta and R. L. Sugar, *Phys. Rev. D* **3**, 970 (1971); B. Hasslacher and D. K. Sinclair, *ibid.* **3**, 1770 (1971).

¹⁶R. Blankenbecler and H. M. Fried, *Phys. Rev. D* **8**, 678 (1973).

¹⁷J. A. Skard and J. R. Fulco, *Phys. Rev. D* **8**, 312 (1973).

¹⁸For every diagram drawn in this paper, one must add a sum over all possible ways of attaching the exchanged mesons to the world lines of the incident particles.

¹⁹H. M. Fried, *Phys. Rev. D* **3**, 2010 (1971).

²⁰For the moment we neglect the couplings between the various meson channels.

²¹J. Botke, D. J. Scalapino, and R. L. Sugar, UCSB report (unpublished).

²²This simplification is by no means essential. See Refs. 1-5 and 17.

²³In general the indices k and l can be continuous.

²⁴R. C. Hwa, *Phys. Rev. Lett.* **26**, 1143 (1971); M. Jacob and R. Slansky, *Phys. Rev. D* **5**, 1847 (1972).

²⁵One of the first papers to evaluate the contribution of vector-meson exchange and fragmentation is that of S. Berman and M. Jacob [*Phys. Rev. Lett.* **25**, 1683 (1970)], who found a logarithmically increasing contribution to the total cross section. See also the recent work connecting growing total cross sections to the triple-Regge coupling by A. Capella, Min-Shih Chen, M. Kugler, and R. D. Peccei, *ibid.* **31**, 497 (1973); G. F. Chew, *Phys. Lett.* **B44**, 169 (1973); M. Bishari and J. Koplik, *ibid.* **B44**, 175 (1973); W. R. Frazer, D. R. Snider, and C.-I. Tan, *Phys. Rev. D* **8**, 3180 (1973). Some of the effects of absorption are treated by D. Amati, L. Caneschi, and M. Ciafaloni, *Nucl. Phys.* **B62**, 173 (1973), but they do not include the

graphs which reverse the sign of the triple-Pomeron term. On the other hand, T. N. Ng and V. P. Sukhatme [University of Washington report, 1973 (unpublished)] use Gribov's Regge calculus with decoupling and find a negative contribution to the total cross section and also an excellent fit to the data.

²⁶V. N. Gribov, Zh. Eksp. Teor. Fiz. 53, 654 (1967) [Sov. Phys.—JETP 26, 414 (1968)]. See also S. Mandelstam, Nuovo Cimento 30, 1127 (1963); 30, 1143 (1963), and A. R. White, Nucl. Phys. B37, 432 (1968); B37, 461 (1968).

²⁷I. G. Halliday and C. T. Sachrajda, Imperial College Report No. ICTP/72/16 (unpublished). For an excellent review of this subject see A. R. White, CERN Report No. TH-1646, presented to the Eighth Rencontre de Moriond, Meribel-les-Allues, 1973 (unpublished); T. L. Neff, Phys. Lett. 43B, 391 (1973).

²⁸H. D. I. Abarbanel, G. F. Chew, M. L. Goldberger, and L. M. Saunders, Phys. Rev. Lett. 26, 937 (1971).

For further references and a review and critique of these papers, see T. L. Neff, Berkeley Report Nos. LBL 1767 and 2003, 1973 (unpublished), and J. Botke, Phys. Rev. D 8, 2584, 2594 (1973).

²⁹A. Mueller, Phys. Rev. D 2, 2963 (1970).

³⁰These interactions can be easily pictured in impact-parameter space. If the simple multiperipheral graph is represented as a chain in this space which stretches between the target and projectile, then the absorptive graphs arise from interactions which occur between the ends of the chain, between one end and somewhere along the chain, and between two points along the chain. Absorption therefore clearly suppresses those configurations in which the chain is coiled up on itself—it prefers to be as straight as possible. One important effect of this phenomenon is to modify the distribution in the variables conjugate to the impact parameters—namely, the relative transverse momenta.

PHYSICAL REVIEW D

VOLUME 9, NUMBER 3

1 FEBRUARY 1974

Decay $L^0 \rightarrow \nu_l \gamma$ in gauge theories of weak and electromagnetic interactions*

Robert Shrock†

Joseph Henry Laboratories, Princeton University, Princeton, New Jersey 08540

(Received 4 September 1973)

Results are presented of a calculation of the rate for the decay $L^0 \rightarrow \nu_l \gamma$, where $L^0 = E^0$, M^0 is a neutral heavy lepton occurring in certain gauge theories of weak and electromagnetic interactions. This rate is compared with that for the semileptonic decay mode $L^0 \rightarrow l^- \pi^+$, and it is found that, although the former is of order α^3 , whereas the latter is of order α^2 , the $L^0 \rightarrow \nu_l \gamma$ rate can actually exceed the $L^0 \rightarrow l^- \pi^+$ rate in models which also have a charged heavy lepton L^+ .

Non-Abelian gauge theories of weak and electromagnetic interactions employing the Higgs-Kibble mechanism of spontaneous symmetry breaking have evoked considerable interest since they provide a natural unification of these two classes of interactions and make possible a renormalizable theory of weak interactions.¹ Heavy leptons play an important role in such theories, being required in models which either do not have the neutral massive gauge boson Z , or have it but do not couple it to a $\bar{\nu}_l \gamma_{\alpha} \frac{1}{2} (1 - \gamma_5) \nu$ neutral current.² Several models feature a neutral heavy lepton $L^0 = E^0, M^0$; these include the Georgi-Glashow (GG) model,³ the second Prentki-Zumino (PZ) model,⁴ and the 2-2, 3-2, and 2-3 models of Bjorken and Llewellyn Smith (B-LS).⁵

In this paper we calculate the rate for the decay $L^0 \rightarrow \nu_l \gamma$ in these five models. For definiteness we consider the heavy muon lepton M^0 ; our results apply equally well to the E^0 . This decay is of interest, first, because, being completely leptonic, it is exactly calculable and independent

of assumptions about how hadrons are included in the various models. Second, experimentally, in view of the difficulty of observing the final particles in the $L^0 \rightarrow \nu_l \gamma$ decay, one would like to determine how large the rate is, especially in comparison with the more easily observed charged modes. Since the GG model embodies the essential characteristics of a theory with heavy leptons, we concentrate on it and give only final results for the other models considered.

A brief review of the particle content of these theories may be helpful. The GG model is based on the group $O(3)$ and has as gauge particles the charged intermediate vector bosons W^{\pm} and the photon γ , but not the neutral gauge boson Z . The scalar fields form a self-conjugate triplet representation of $O(3)$,

$$\begin{pmatrix} \phi^+ \\ \phi^0 \\ \phi^- \end{pmatrix}.$$

After the spontaneous symmetry breakdown and